URSI AP-RASC, Sydney, Australia, 17 – 22 August 2025

A Ultra-Wideband Receiver System for Solar Radio Observations

Zhaomin Peng(1)(2), Jun Shi* (1)(2), and Dehai Zhang(1)(2)
(1) Key Lab of Microwave Remote Sensing, National Space Science Center
(2) Chinese Academy of Sciences，Bei Jing，China

Abstract

Solar radio emissions offer critical insights into dynamic processes within the Sun's atmosphere, including coronal heating, solar eruptions, and the generation of the solar wind. This paper introduces an ultra-wideband receiver system operating across a broad frequency range, specifically engineered for high-sensitivity observations of both thermal and non-thermal solar emissions. Our system integrates low-noise amplifiers, multi-band filters, frequency down-conversion mixers, wideband spectrometers, and a built-in noise source to achieve high temporal and frequency resolution. The addition of the internal noise source enables real-time calibration of system noise during observations. This enhanced capability allows for comprehensive studies of dynamic solar phenomena such as transition region small-scale microwave bursts. Preliminary experimental results confirm the system’s ability to capture transient radio emissions, providing a solid foundation for future solar physics research.

1. Introduction

The Sun, as the closest star to Earth, is a dynamic and highly active celestial body. Its various atmospheric layers, particularly the solar transition region and corona, are key to understanding fundamental astrophysical processes such as coronal heating, solar eruptions, and the generation of solar wind[1]. Solar radio emissions, which are produced through the interaction of energetic particles with magnetic fields in the solar atmosphere, provide invaluable insights into these phenomena.

The transition region lies between the solar chromosphere and the corona, representing a thin but highly dynamic layer where a rapid increase in temperature occurs. This region experiences dramatic gradients in temperature, density, and magnetic field strength, making it an active site for various physical processes. The temperature in the transition region rises sharply from approximately 20,000 K in the upper chromosphere to nearly a million K at the base of the corona, leading to intense plasma dynamics and energetic particle interactions. These processes are critical to understanding solar phenomena, such as coronal heating and the initiation of solar flares and coronal mass ejections (CMEs)[2].

Observations of the Sun across various wavelengths, including ultraviolet (UV) and extreme ultraviolet (EUV), have provided a wealth of information about thermal processes occurring in the solar atmosphere[3]. These observations have shed light on the behavior of small-scale features such as spicules, jets, and bright points, which are associated with thermal processes in the transition region. However, to fully comprehend the complex dynamics of the solar transition region, it is essential to observe not only thermal processes but also non-thermal phenomena.

Non-thermal processes in the Sun, such as magnetic reconnection and turbulence, can accelerate electrons to high energies, which subsequently produce radio emissions through mechanisms such as gyro synchrotron radiation. These non-thermal radio emissions, including small-scale microwave bursts in the transition region, are crucial for understanding energy release mechanisms and the behavior of energetic particles in the Sun’s atmosphere[4]. These bursts are typically short-lived, narrowband, and characterized by rapid frequency drifting, making them particularly valuable for probing the dynamic processes occurring in the solar transition region.

To effectively study non-thermal emissions, a high-sensitivity, broad-frequency receiver is essential to bridge the existing observational gap. Our ultra-wideband system provides the required temporal and spectral resolution to capture rapid, transient solar radio bursts, facilitating a more detailed investigation of energy dissipation and particle acceleration in the transition region and corona. Current radio telescopes, especially those operating in the millimeter-wave frequency range, are hindered by significant atmospheric interference, particularly high-frequency region where substantial solar activity occurs[5]. Many of these systems suffer from limited intermediate frequency (IF) bandwidth, often unable to capture the full range of solar emissions. In contrast, the system presented here achieves a wider IF bandwidth(7GHz), enabling high-resolution observations and providing a more complete and detailed study of solar phenomena within this critical frequency range. This underscores the need for advanced instruments capable of high temporal and frequency resolutions to provide accurate measurements of non-thermal radio emissions linked to solar activity.

The development of a ultra-wideband receiver system for solar radio observations, designed to capture emissions in the 15-36 GHz range, provides a promising solution to address these challenges. Such a system can significantly enhance our ability to observe and analyze non-thermal processes in the solar transition region, providing valuable insights into solar dynamics and energy transport mechanisms. By offering broad frequency coverage, this receiver system could contribute to advancing the field of solar physics and space weather studies, improving our understanding of the Sun's behavior and its impact on the Earth’s space environment.

2. System Experimental Design

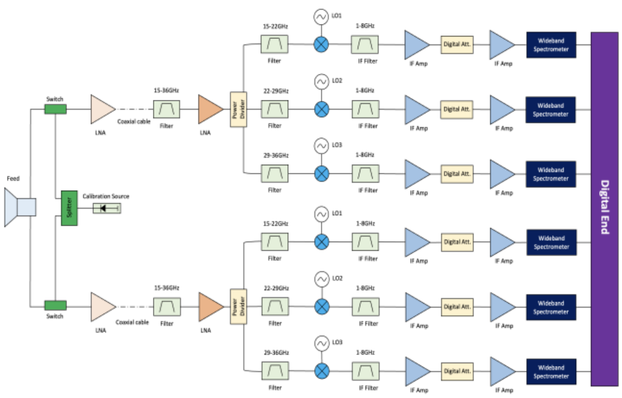

Figure 1. Block diagram of the ultra-wideband receiver system for solar radio observations, illustrating the signal reception, amplification, frequency conversion, and spectral analysis components.

As illustrated in Figure 1, the receiver system is designed to observe solar radio emissions across an ultra-wideband frequency range of 15-36 GHz. The system incorporates a dual-channel architecture, where each channel is equipped with a built-in noise source, facilitating real-time noise calibration during observations. The use of a quadruple-ridged flared horn as the feed antenna enables the system to achieve a significantly broader bandwidth for signal reception when compared to conventional radio observation systems utilizing corrugated horn antennas. This design enhances the system’s capacity to capture a wider frequency spectrum, thereby improving its ability to detect high-frequency solar emissions. Moreover, the intermediate frequency bandwidth extends up to 7 GHz, spanning the 1-8 GHz range, which ensures both high temporal and frequency resolution. This configuration facilitates comprehensive studies of solar phenomena while maintaining optimal performance across the entire operational frequency range. The system's signal reception begins with the feed antenna, which is coupled to a Low Noise Amplifier (LNA) to amplify the weak incoming signals.

The LNA ensures the amplification of weak incoming signals while minimizing system noise, maintaining the fidelity of the signal for further processing. The system noise figure is determined by the amplifier cascade principle：

$$NF = F_1 + \frac{F_2 - 1}{G_1} + \frac{F_3 - 1}{G_1 G_2} + \cdots + \frac{F_n - 1}{G_1 G_2 \ldots G_{n-1}} \qquad (1)$$

F_n represents the noise factor of the nth stage， G_{n-1} represents the gain of the (n-1)th stage, and NF represents the noise figure of the entire system. According to (1), we utilize an LNA as the first stage in the receiving section to amplify the received signal. The high gain and low-noise performance provided by this amplifier can effectively reduce the contribution of subsequent cascaded device noise coefficients to the overall noise. After initial amplification, the signal is passed through a series of filters designed to isolate the desired frequency bands (15-22 GHz, 22-29 GHz, and 29-36 GHz). These filters remove unwanted frequencies, thus enhancing the quality of the signal by preventing interference from out-of-band signals. The filtered signal is routed through a Power Divider to distribute it across multiple channels. Each channel is equipped with a local oscillator (LO) that generates a frequency suitable for mixing with the received signal. This mixer performs frequency conversion, translating the received high-frequency signal to a lower intermediate frequency (IF), which is easier to process in subsequent stages. The mixed signals are then passed through IF Filters, which further clean the signal by eliminating unwanted high-frequency components. The filtered signals are subsequently amplified by IF Amplifiers to ensure sufficient signal strength for analysis. Each channel is equipped with a Digital Attenuator that allows precise control over the signal’s gain, optimizing the system’s dynamic range and preventing signal saturation. The processed signals are directed to the Wideband Spectrometer, which performs spectral analysis on the solar radio emissions.

This spectrometer enables the capture of detailed frequency data, essential for identifying transient radio bursts, especially those associated with non-thermal processes in the solar transition region and corona. The spectrometer provides real-time measurements of frequency drift rates and burst characteristics, crucial for studying phenomena such as Transition Region Small-Scale Microwave Bursts (TR-SMBs). The following Figure.2 is the detailed physical image of the feed antenna, reflector antenna, and several key components.

(a) (b)

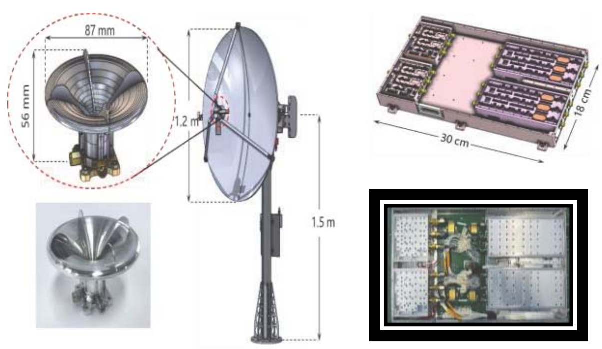

Figure 2. (a) Structural diagram of feed antenna and reflector antenna size. (b) Dimensional structure diagram of ultra-wideband receiver.

This spectrometer enables the capture of detailed frequency data, essential for identifying transient radio bursts, especially those associated with non-thermal processes in the solar transition region and corona. The spectrometer provides real-time measurements of frequency drift rates and burst characteristics, crucial for studying phenomena such as TR-SMBs. The following Figure.2 is the detailed physical image of the feed antenna, reflector antenna, and several key components.

3. Results and Discussion

Figure 3. Align the antenna with the sun for overall system testing

We chose to test the system indoors like figure 3, measuring the overall receiver's noise figure, aligning the entire system with the sun and testing the gain of each channel. The final results are shown in Figure 3.

(a)

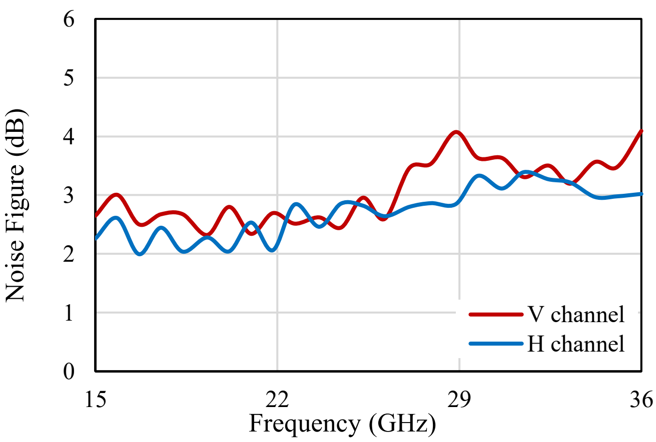

(b)

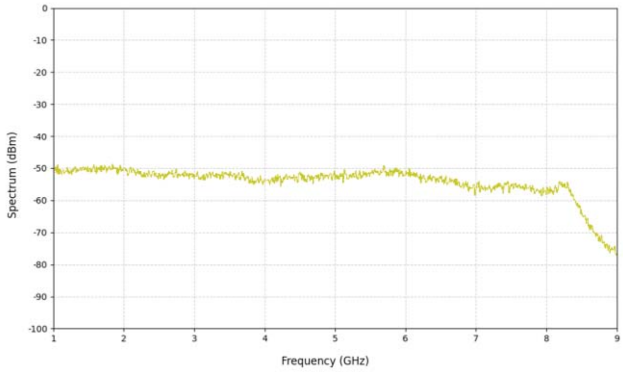

(c)

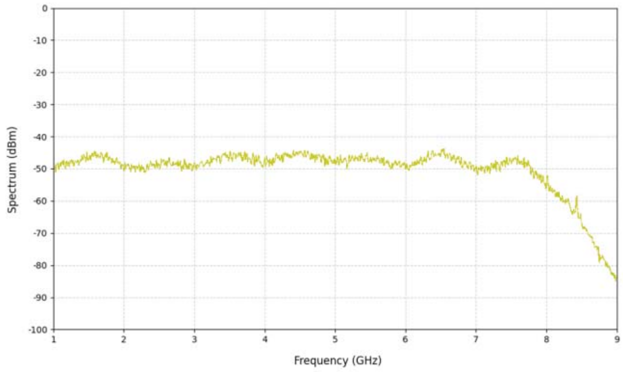

(d)

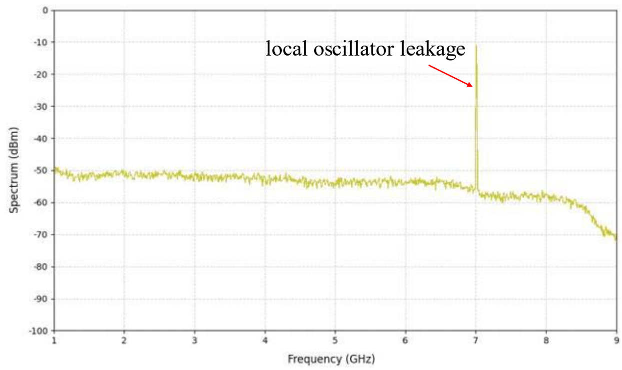

Figure 4. (a) The overall receiver's noise figure. (b)-(d) The spectrum of H channel(1-3).

The experimental performance of the multi-channel receiver system demonstrates its high sensitivity and stability in detecting solar radio emissions within the 15-36 GHz frequency range. The system achieves a consistently low noise figure across both channels, with performance optimized in the 15-25 GHz range, where the noise figure remains below 3 dB. Specifically, Figure 4(a) illustrates the noise figure measurements, showing values consistently under 4 dB across the tested frequency range, with a marked improvement in the 15-25 GHz band. This suggests that the system effectively minimizes noise contributions, especially in critical observational bands where solar activity is most prevalent.

The system's passband remains flat across the 1-8 GHz range, as demonstrated in Figure 4(b)-(d), which show the gain measurements across multiple frequencies. This flat passband is crucial for ensuring signal integrity, particularly when capturing transient solar radio bursts that can span a wide frequency range. The flatness of the passband indicates the system's ability to maintain stable performance across a broad spectrum, which is essential for observing dynamic solar events such as solar flares and small-scale microwave bursts. Such stability in the passband enhances the accuracy of measurements and ensures that no unwanted signal distortion occurs during the collection of solar radio emissions.

However, a signal peak was observed at higher frequencies, particularly in the Figure 4(d) H3 channel, which was identified as a result of local oscillator leakage. As illustrated in Figure 4(d), this peak interferes with the overall signal integrity, causing distortions that could potentially compromise data quality. The leakage of the LO signal into the observed frequency path introduces spurious peaks that are not representative of the solar emissions under study.

To address this challenge, we consider enhancing isolation between the LO and IF stages through the implementation of advanced filtering and shielding techniques. Additionally, we will experiment with modifying the LO signal generation to minimize leakage, ensuring that the signal path remains unaffected by unwanted interference. These improvements will significantly enhance the signal quality, particularly in the higher frequency bands where transient events such as solar flares are most prominent.

Despite this challenge, the system shows considerable promise for high-quality solar observations, particularly in detecting non-thermal emissions such as small-scale microwave bursts and other rapid, transient events in the solar transition region and corona. These emissions are critical for understanding solar phenomena like magnetic reconnection, particle acceleration, and energy dissipation.

One of the key strengths of the system is its broad frequency coverage and the ability to perform simultaneous multi-frequency observations. This capability significantly enhances the system's utility, allowing for comprehensive studies of solar dynamics and enabling a more detailed investigation of transient solar events across multiple frequency bands. Simultaneous multi-frequency observations offer crucial insights into the complex solar processes occurring in various atmospheric layers, such as solar flares and CMEs.

4. Conclusion

In this paper, we present an ultra-wideband receiver system designed for high-sensitivity solar radio observations. The system operates in the 15-36 GHz range and is optimized to capture non-thermal emissions from the solar transition region and corona. The system features dual-polarization channels with a built-in noise source, enabling real-time calibration of system noise during observations. Additionally, the system's intermediate frequency bandwidth reaches up to 7 GHz, providing enhanced temporal and frequency resolution. Preliminary results demonstrate its ability to observe transient radio bursts.

In the next phase, we will conduct further calibration experiments to enhance measurement accuracy and implement array-based observations for increased spatial resolution. These improvements will enable us to observe finer-scale details of solar emissions and advance our understanding of solar dynamics and space weather. The built-in noise source will continue to ensure real-time calibration, improving the precision and reliability of our measurements. Expanding the number of receivers in the array will increase the system's flexibility, enhancing observational capabilities and providing higher spatial resolution. Array observations will allow for more refined spatial and temporal resolution, facilitating the discovery of new experimental phenomena and deeper insights into solar activity."

References

[1] J. C. Allred, S. L. Hawley, W. P. Abbett, and M. Carlsson, "Radiative Hydrodynamic Models of the Optical and Ultraviolet Emission from Solar Flares," *The Astrophysical Journal*, vol. 630, no. 1, p. 573, 2005/09/01 2005, doi: 10.1086/431751.

[2] K. K. Reeves, T. Török, Z. Mikić, J. Linker, and N. A. Murphy, "Exploring Plasma Heating in the Current Sheet Region in a Three-dimensional Coronal Mass Ejection Simulation," The Astrophysical Journal, vol. 887, no. 1, p. 103, 2019/12/13 2019, doi: 10.3847/1538-4357/ab4ce8.

[3] M. J. Aschwanden et al., "Global Energetics of Solar Flares. V. Energy Closure in Flares and Coronal Mass Ejections," *The Astrophysical Journ*al, vol. 836, no. 1, p. 17, 2017/02/06 2017, doi: 10.3847/1538-4357/836/1/17.

[4] A. K. Verma, J.-L. Margot, and A. H. Greenberg, "Prospects of Dynamical Determination of General Relativity Parameter β and Solar Quadrupole Moment with Asteroid Radar Astronomy," *The Astrophysical Journal*, vol. 845, no. 2, p. 166, 2017/08/23 2017, doi: 10.3847/1538-4357/aa8308.

[5] Z. Shang et al., "A Broadband Solar Radio Dynamic Spectrometer Working in the Millimeter-wave Band," *The Astrophysical Journal Supplement Series*, vol. 258, no. 2, 2022, doi: 10.3847/1538-4365/ac4257.